

Aggregate production: Fines generation during rock crushing

M.S. Guimaraes ^a, J.R. Valdes ^b, A.M. Palomino ^{c,*}, J.C. Santamarina ^d

^a *Aalborg Portland, Denmark*

^b *Department of Civil and Environmental Eng., San Diego State University, San Diego, CA 92182, USA*

^c *Department of Civil and Environmental Eng., Penn State University, University Park, PA 16802, USA*

^d *Civil and Environmental Engineering, Georgia Institute of Technology, Atlanta, GA 30332, USA*

Received 4 May 2006; received in revised form 7 August 2006; accepted 16 August 2006

Available online 25 September 2006

Abstract

The energy required to crush rocks is proportional to the amount of new surface area that is created; hence, a very important percentage of the energy consumed to produce construction aggregates is spent in producing non-commercial fines. Data gathered during visits to quarries, an extensive survey and laboratory experiments are used to explore the role of mineralogy and fracture mode in fines production during the crushing of single aggregates and aggregates within granular packs. Results show that particle-level loading conditions determine the failure mode, resulting particle shape and fines generation. Point loading (both single particles and grains in loose packings) produces clean fractures and a small percentage of fines. In choked operations, high inter-particle coordination controls particle-level loading conditions, causes micro-fractures on new aggregate faces and generates a large amount of fines. The generation of fines increases when shear is imposed during crushing. Aggregates produced in current crushing operations show the effects of multiple loading conditions and fracture modes. Results support the producers' empirical observations that the desired cubicity of aggregates is obtained at the expense of increased fines generation when standard equipment is used.

© 2006 Elsevier B.V. All rights reserved.

Keywords: Crushed stone; Cubicity; Sand; Crushing; Aggregates; Fracture modes; Mineralogy; Fines

1. Introduction

The absence of natural aggregate at cost-effective transportation distances has prompted extensive use of manufactured aggregates. The US aggregate industry produces ~1.1 billion tons of crushed stone per year with carbonates and granites accounting for 71% and 16%, respectively (USGS, 2000). The extensive use of manufactured aggregates has required proper modification of characterization, design and construction prac-

tices. In addition, it has motivated studies to reduce energy consumption, to attain optimal crusher design and operation, and to minimize waste.

Aggregate manufacturing typically starts by blasting rock masses and is followed by a series of crushing stages. Comminution in typical hard rock quarries is sketched in Fig. 1. ASTM particle size distributions of select aggregate products are also shown in Fig. 1 (ASTM, 2000). Crushing operations can accommodate some adjustment to match the demand for each gradation.

Crushers used for hard rock are sketched in Table 1. The table also includes data gathered as part of this study, including: typical reduction ratios (the ratio between the sieve opening for 50% of the feed and for 50% of the

* Corresponding author. Tel.: +1 814 865 9427; fax: +1 814 863 7304.

E-mail address: amp26@psu.edu (A.M. Palomino).

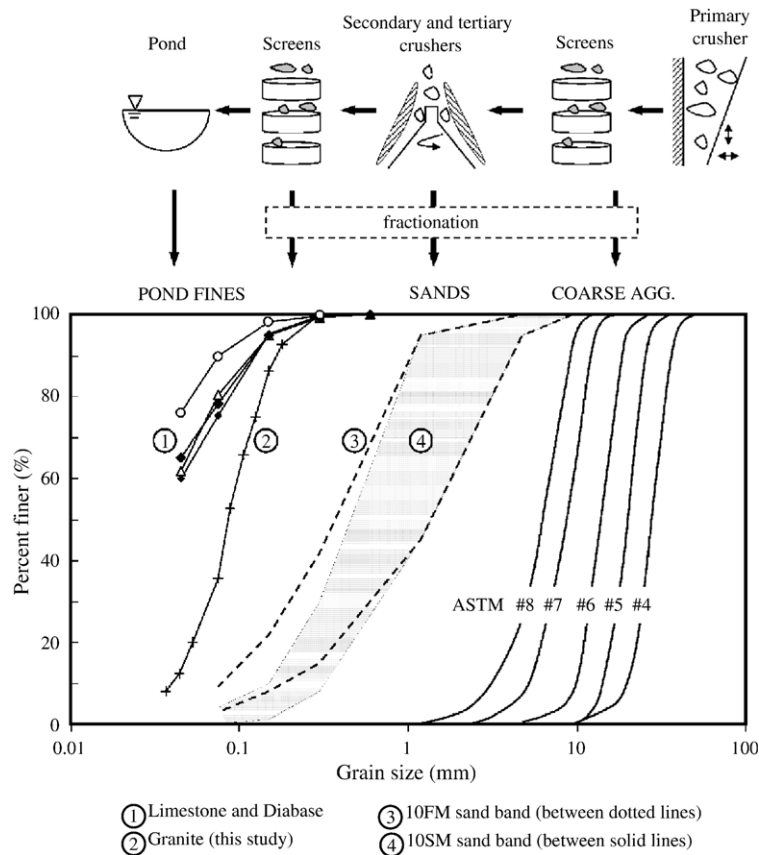


Fig. 1. Schematic diagram of a typical comminution process and end-product grain size distributions. Limestone and diabase data from Wood and Marek (1996).

product) and the average percentage of fines generated from each crusher type. Two heuristics guide most crushing operations: (1) lower reduction ratios reduce fines generation and (2) choke-feeding the crushers produces better shaped aggregate but more fines.

Fines that do not meet minimum particle size requirements for use in concrete find little use and remain stockpiled (in Georgia, these fines account for approximately 4% of the total aggregate production). In addition, there is virtually no use for pond screenings that are obtained after washing the different gradations, in particular manufactured sand (Wood and Marek, 1996; Collins et al., 1997). Therefore, two current trends exacerbate the situation with unused fines (stockpiles exceed 20 million tons in Georgia alone). First, there is increased demand for manufactured sand, which already accounts for approximately 12% of crushed stone consumption (USGS, 2000). Second, there is increased demand on cubicity, and standard comminution practices improve cubicity by imposing additional crushing or abrasion, which leads to increased fines generation.

The purposes of this study are to explore the role of mineralogy and crushing mode on fines production and resulting particle shape. These topics are studied with a combination of data gathered during visits to quarries, an extensive mail-in survey and laboratory experiments. (Note: within the context of this manuscript, the term “fines” refers to particles that pass the #200 sieve.)

2. Fines generation and mineralogy

Information about crushing sequence, fines production, mineralogy and mechanical properties of granites were collected from a survey of 35 quarries in Georgia. Granite specimens in the area contain orthoclase, quartz, plagioclase and biotite, often in enough quantity and size to be identifiable by the unaided eye. In the absence of specific mineralogy data, the reported oxides are used as indicators of specific minerals, for example: $\text{SiO}_2 \rightarrow$ quartz, $\text{CaO} \rightarrow$ anorthite, $\text{K}_2\text{O} \rightarrow$ orthoclase and high contents of Fe_2O_3 and $\text{MgO} \rightarrow$ biotite.

Table 1
Crushers and production characteristics

Crusher type	Primary crushers		Secondary and tertiary crushers
	Jaw	Gyratory	Cone
Main purpose	Size reduction		Size reduction, cubicity and breakage of microfractured particles
Production line	<i>Open circuit</i>		<i>Secondary: open circuit, tertiary: closed circuit</i>
Reduction ratio	2:1 to 10:1 <i>3:1 to 7:1</i>	3:1 to 10:1	2:1 to 8:1 <i>2:1 to 6:1</i>
Fines <0.075 mm (percentage of feed)	3.5%	4.7%	<i>Secondary: 1.1%, tertiary: 1.6–1.9%</i>

Input in italics: gathered from 35 granite quarries in Georgia as part of this study. About 60% of the primary crushers are jaw crushers. Impact crushers are used for softer rocks such as limestone. Wet crushing lowers capacity and improves shape (particles stay longer within the crusher and experience more loading cycles). Only 1 of the 35 surveyed quarries operates under wet conditions.

Other sources: McNally (1998), Heikkila (1991) and Bowers et al. (1996).

The specific gravity of granite-forming minerals follows: quartz $G_s=2.65$, orthoclase $G_s=2.67$, mica $G_s=2.82$ and anorthite $G_s=2.76$. Therefore, granites with high specific gravity are rich in either biotite or anorthite. Survey data plotted in Fig. 2a show the relation between specific gravity and silica and iron oxide contents.

Fig. 2b shows reported LA abrasion breakage values versus oxide content. Although there is a weak correlation between abrasion breakage and the mineralogy of granites, the data suggest that quartz (indicated by SiO_2) with a Mohs hardness of 7 increases rock degradation probably by crushing weaker minerals during the LA abrasion test. On the other hand, the

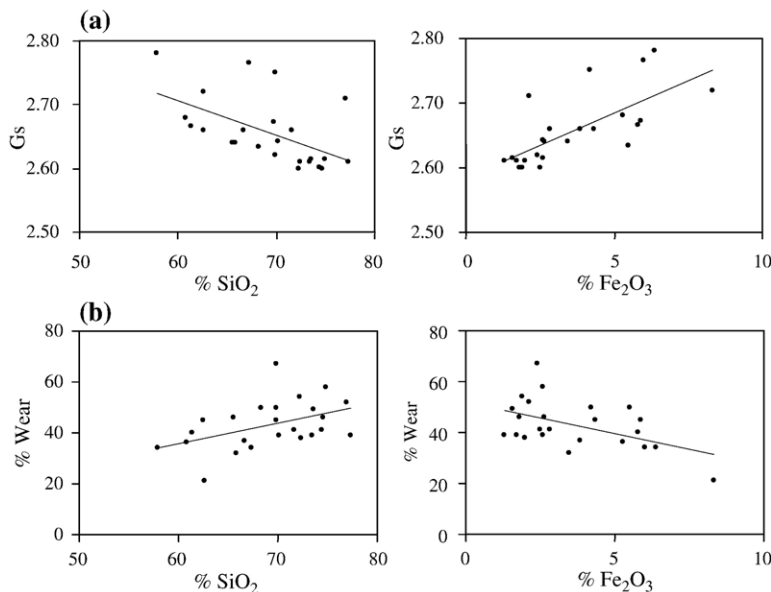


Fig. 2. Relationship between (a) oxide content and specific gravity and (b) percent wear in LA abrasion tests.

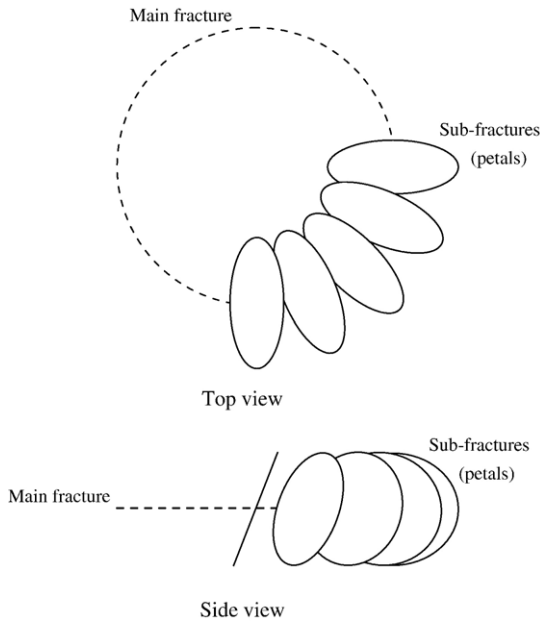


Fig. 3. Mixed mode fracture surfaces exhibit multiple transverse petal-like fractures inclined with respect to the plane of the main mode I fracture.

presence of biotite (indicated by Fe_2O_3) decreases the amount of wear in the LA abrasion test, probably by creating a cushioning effect that reduces impact stresses and wear. The presence of anorthite and orthoclase—inferred from CaO and K_2O —does not influence the percentage wear in the LA abrasion test (data not shown here).

Finally, there is no correlation between the amount of pond screenings that were reported and the parameters considered above, including the content of various oxides (i.e., mineralogy), specific gravity and LA abrasion. Therefore, differences in mineralogy among the various granites in the area play a secondary role in defining the amount of generated fines. The next two

sections focus on the effect of crushing conditions on fines generation.

3. Single particle crushing

Crushers break rocks by fracture propagation induced by the applied compression and shear forces. The theoretical bases for fracture mechanics started in 1921 when Griffith related fracture propagation to pre-existing cracks or defects. Later, in 1957, Irwin introduced the concept of stress intensity to assess fracture propagation and suggested that a fracture propagates when the stress intensity factor approaches a critical value that is characteristic for each material. The stress intensity varies with the fracture mode; there are three primary modes: ‘mode I’ (opening) is due to normal tensile stress and ‘mode II’ (sliding) and ‘Mode III’ (tearing) are due to in-plane shear. In most cases, loading conditions produce mixed-mode fracture propagation. Mixed mode fracture surfaces, such as mode II superposed on mode I, exhibit multiple transverse fractures that look like flower petals inclined with respect to the planar surface produced by the mode I fracture (experiments conducted in collaboration with L. Germanovich—Fig. 3).

Granites are made of different mineral grains; hence, there are interfaces. The failure in cohesive granular materials is intrinsically related to the presence of microcavities and the stiffness contrast between components. Pores (width-to-length ratio $>10^{-1}$ to 1) are less harmful than cracks (width-to-length ratio $<10^{-1}$). Cracks account for 15% to 36% of the total porosity in granites and their length in unstressed granites ranges between 10% and 20% of the grain size (Sprunt and Brace, 1974). Cracks in granites are most commonly found at grain boundaries, and might have originated from internal stresses caused by changes in pressure and temperature. In addition, low aspect ratio cracks are

Dynamic longitudinal compression	Static longitudinal compression	Static diagonal compression	Brazilian Test	3-point short beam
0.5% to 4%	1% to 2%	0.1% to 0.3%	0.05% to 0.4%	0.05% to 0.08%

Fig. 4. Fines generated under different loading mechanisms. Specimens prepared with mixtures of gypsum and sand.

found along cleavage planes on micas and feldspars, albeit less frequently (Tapponier and Brace, 1976).

When a compressive load is first applied, the randomly oriented cracks tend to close. If the load is increased, the faces of the microcavity slide relative to each other. This displacement produces tensile stresses at the tips, causing the fracture to propagate in tension in the direction of the load. The interaction between neighboring cracks alters the stress field and the original propagation path of a fracture (Kranz, 1979; Gramberg, 1989; Vasarhelyi and Bobet, 2000; Germanovich et al., 1996).

The previous observations suggest that fracture propagation is closely related to the internal structure and mechanical properties of rock grains and minerals. For instance, dense, fine-grained rocks such as limestone develop very straight needle-shaped fractures that propagate without interacting with each other leading to an explosive failure (Gramberg, 1989). However, marble, with the same mineralogy as limestone but with

coarse weakly cemented grains, develops multiple macroscopic fractures that aggregate in shear bands. In addition, the plastic deformation of calcite grains reduces the stress concentration at the crack tip, the crack expands laterally and crack propagation is hindered. Consequently, the size and mechanical properties of calcite generate two very different failure mechanisms in limestone and marble. In the case of granite, quartz and feldspar grains do not deform plastically at low confinement, and crack propagation continues in the direction of the applied load (Gramberg, 1989). Hence, granite and marble—both coarse-grained rocks with planar pre-existing cracks—fail very differently.

3.1. Experimental study

Preliminary laboratory tests on the influence of the loading conditions on cohesive materials were conducted with gypsum specimens. Sand was mixed in the gypsum paste to model a material with some internal granularity

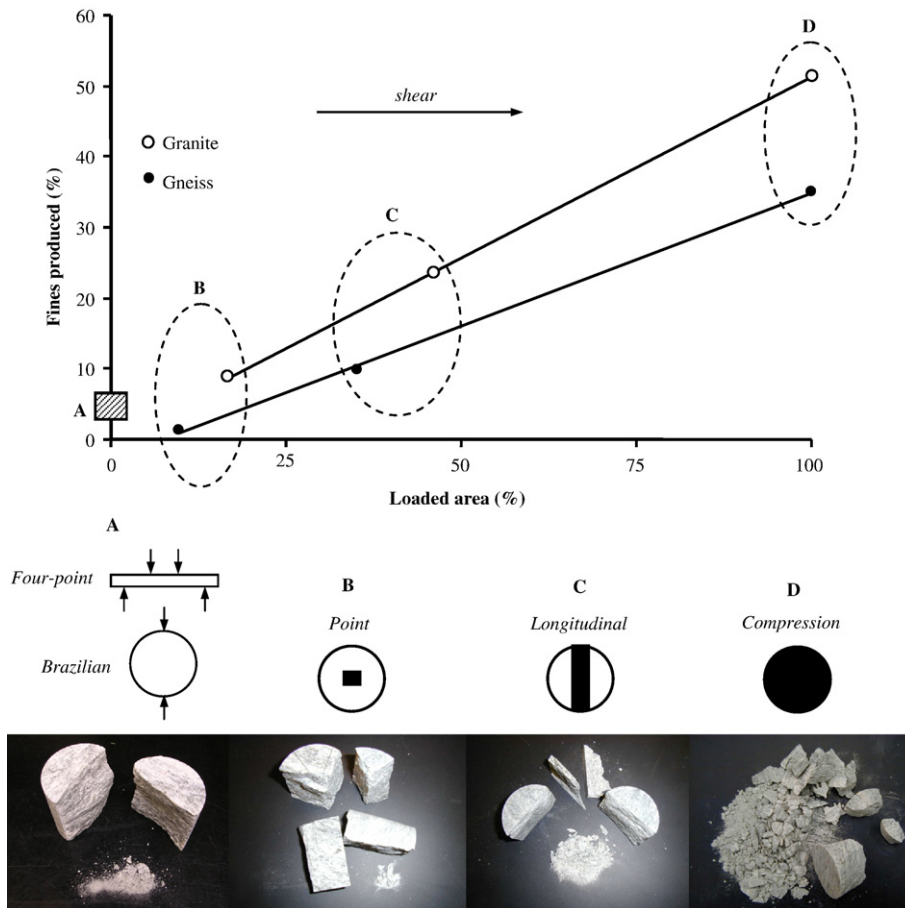


Fig. 5. Fines generated in axially loaded specimens versus the relative size of the loaded area. The shaded box “A” represents the tensile tests for both granite and gneiss.

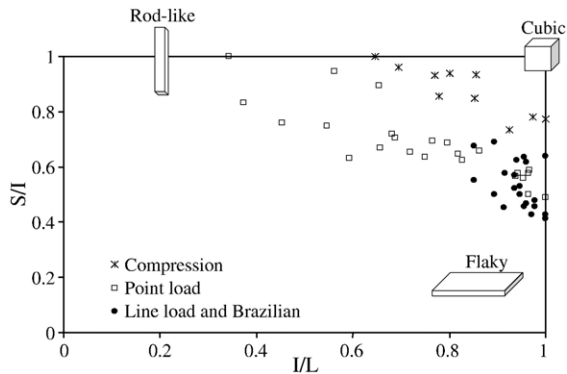


Fig. 6. Shape index for aggregates from each type of test on granite and gneiss specimens (I=intermediate axis length; L=long axis length; S=short axis length).

and stiffness contrast. The various load configurations and corresponding results are summarized in Fig. 4. Longitudinal compression produced the highest amount of fines, while load configurations that promoted tensile failure caused the least amount. Additional gypsum specimens without sand were tested under similar conditions and show less fines generation. These results highlight: (1) the role of interfaces on fines generation, which cannot be controlled for a given rock, and (2) the importance of loading mode, which can be partially controlled through crusher design and operation.

The effects of load configuration were studied further with granite specimens. Cores of granite ($G_s=2.65$, core diameter $d=36$ mm—Greene County, Georgia) and gneiss ($G_s=2.64$, core diameter=47 mm from Buford, Georgia) were subjected to different loading configurations. Brazilian tests and four-point flexural tests were performed to evaluate the amount of fines generated in relatively pure mode I failure. For these tests, specimen aspect ratios ranged from 5.3 to 6.5. Compression loads were applied to cylindrical specimens with length-to-diameter ratios ranging between 0.9 and 1.0, and repeated for different sizes of the loading area: point load, line load and full face. These loading configurations are sketched with labels A, B, C and D in Fig. 5. Three specimens were tested for each load configuration (see Guimaraes, 2002 for test details and the complete dataset).

3.1.1. Fines generation

Results are summarized in Fig. 5. The four-point flexural test generated no significant fines and the specimens subjected to the Brazilian test generated some fines, primarily at the contact between the loading device and the rock. On the other hand, the axially loaded tests produced significant amounts of fines and

the amount of fines generated increased with increasing loaded area.

3.1.2. Characteristics of fracture surfaces

The fracture faces that formed during the four-point flexural test and the Brazilian test were rough and clean, there was no evidence of attrition powder, fractures developed along grain boundaries, and both cleavage fractures in biotite and feldspars and conchoidal fractures in quartz were easily identifiable on fracture faces. However, fracture surfaces that resulted from the compression tests were covered with small and shallow transverse cracks (i.e., mixed mode), showed a teeth-like texture, and fine powder on surfaces evidenced the attrition between the coarse aggregates.

3.1.3. Cubicity

The shape of aggregates generated after crushing is assessed in terms of the long L, intermediate I and short S axes (as in Zingg, 1935). Measurements are plotted in terms of ratios S/I and I/L in Fig. 6. Aggregates produced in full-face compression tests show the highest cubicity. Aggregates produced in line-load and Brazilian tests show high degree of flakiness. Aggregates from point-load tests exhibited flaky and rod-like shapes. Finally, the aggregates resulting from the four-point flexural tests showed “improved cubicity”; however, this loading condition can only be applied to aggregates that have high initial slenderness.

3.2. Field and lab comparison

The previous results point to the relevance of shear and mixed failure modes in fines generation. The faces of aggregates sampled from secondary and tertiary crushers during the site visits conducted as part of this study showed both planar surfaces with powder (as observed in compression tests) as well as clean rough surfaces (as observed in tensile tests), often on the same particle. This suggests that multiple loading conditions take place during crushing.

4. Grain crushing in granular packs

Intensive particle-to-particle interaction takes place during crushing operations, particularly when crushers are choke-fed. Crushing of granular packs has been extensively studied in the last two decades. The most important observations relevant to this context are:

- Intersurface coordination plays an important role in the crushing of granular packs. When particles are of

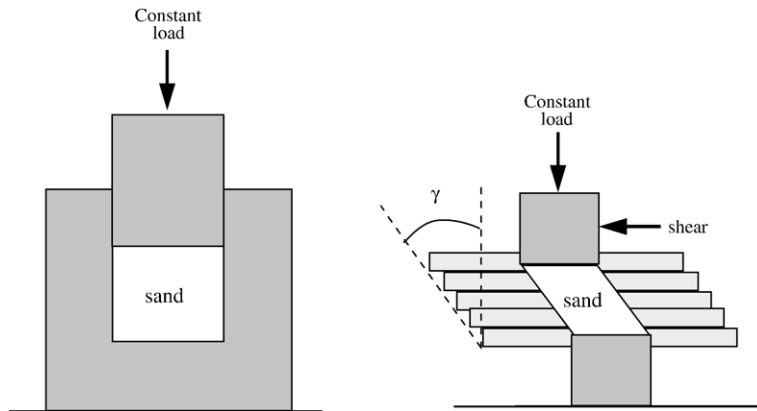


Fig. 7. Devices used to experimentally study particle crushing in granular packings: one-dimensional compression (zero lateral strain) and simple shear.

similar size, the coordination number is low, and they are more likely to be loaded at opposite poles and to experience splitting-type failures. On the contrary, splitting failures are hindered when particles are loaded by smaller size neighbors; the higher coordination number causes a distributed load condition (Heikkila, 1991; McDowell and Daniell, 2001; McDowell and Bolton, 1998).

- The probability of a particle crushing within a granular packing increases with: increasing confining pressure, particle size and particle angularity, and decreasing coefficient of uniformity, density and coordination number (Lee and Farhoomand, 1967; Hardin, 1985; McDowell et al., 1996). In particular, smaller particles in a granular packing generally have lower coordination than the larger ones and have a higher probability of crushing (Coop et al., 2004; McDowell, 1999). Larger particles exhibit abrasion and asperity breakage.
- Particle crushing contributes to volume contraction and reduced dilation in shear (Lee and Seed, 1967; Yamamuro and Lade, 1996). When a granular packing is one-dimensionally loaded, the packing first experiences small deformation (contact deformation followed by some particle rearrangement) until massive crushing begins and elastic yielding takes place (McDowell and Bolton, 1998; Nakata et al., 1999, 2001). The maximum rate of grain crushing occurs near the yield stress, which decreases with decreasing density, and is higher for well-graded materials than for a uniformly graded one at the same relative density (McDowell and Bolton, 1998; Nakata et al., 2001).
- The particle size distribution of the granular material crushed in one-dimensional loading (i.e., zero lateral

strain) often approaches a linear trend on a log-log scale, suggesting a fractal distribution of grain sizes (McDowell, 1999; McDowell and Bolton, 1998; Nakata et al., 2001; Joer et al., 1999; Lobo-Guerrero and Vallejo, 2005).

Given the axial and transverse relative motion of crusher surfaces, further insight is needed into grain crushing when the granular pack is subjected to shear as compared to one-dimensional compression. In addition, data are also needed about the evolution of particle shape. These questions are explored next.

4.1. Experimental study

Two types of loading conditions were implemented: one-dimensional compression and simple shear (devices are shown in Fig. 7). The loose and dense sand specimens were prepared with Ottawa sand (grain

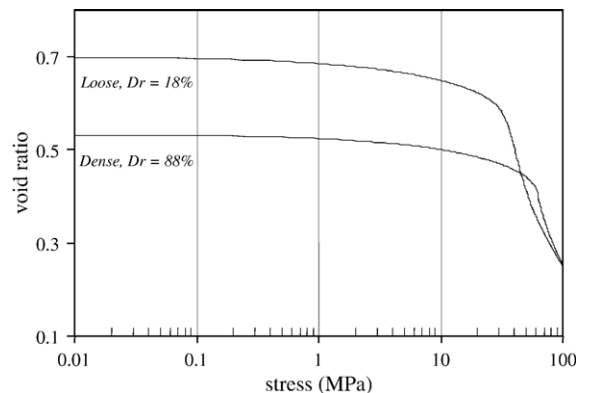


Fig. 8. Load–deformation response in one-dimensional compression (zero lateral strain) for loose and dense packings.

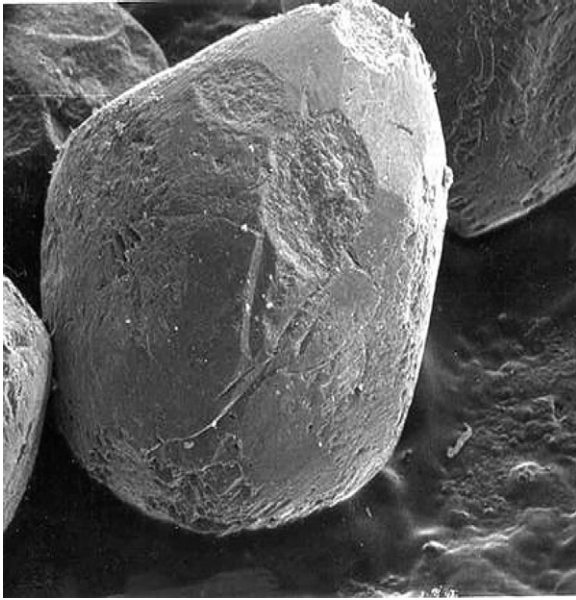


Fig. 9. SEM image of a sand grain obtained from a dense granular specimen subjected to high stresses in one-dimensional compression loading.

diameter between 0.60 mm and 0.85 mm; mean diameter 0.73 mm; minimum void ratio $e_{min}=0.50$ and maximum void ratio $e_{max}=0.74$). Each specimen was repeated three times. The target relative density $D_r=(e_{max}-e)/(e_{max}-e_{min})$ for the dense specimens was $D_r=88\%$ and $D_r=18\%$ for the loose specimens. The axial load was applied with a loading frame. In shear tests, grains were first axially loaded to 14 MPa (the load caused no significant crushing). Shear was then imposed to cause a shear strain $\gamma=18\%$. Additional specimens were loaded to intermediate stress levels to explore the

evolution of crushing. Details and the complete dataset can be found in Valdes (2002).

4.1.1. Load–deformation

Stress vs. void ratio plots for a loose and a dense specimen are presented in Fig. 8. The yield stress for the dense sand is higher than for the loose sand ($\sigma_{y-dense} \sim 60$ MPa, $\sigma_{y-loose} \sim 30$ MPa). The curves cross at about $\sigma \sim 46$ MPa and $e=0.44$ and asymptotically merge at $\sigma > 100$ MPa. However, the grain size distributions obtained at 100 MPa are different for the loose and dense specimens, suggesting different crushing and void-filling mechanisms. Indeed, differences in crushing mode were readily observed under the microscope: particles in the loose packing exhibited splitting and massive breakage, while grains in the dense packing experienced local damage at contacts (Fig. 9).

4.1.2. Fines generation

The grain size distribution curves before and after one-dimensional compression and shear loading are compared in Fig. 10. The loose packing experienced more crushing than the dense packing at all axial loads: $\sigma=14$ MPa, 50 MPa and $\sigma=100$ MPa. The data shows that the application of simple shear caused a major increase in fines generation when the material was already normally loaded near its elastic yield load. In contrast to one-dimensional compression, shearing dense packings may produce more fines than the loose packings.

4.1.3. Microscopy

Fines produced in one-dimensional and simple shear tests were characterized via optical and scanning electron microscopy to gain further insight into the

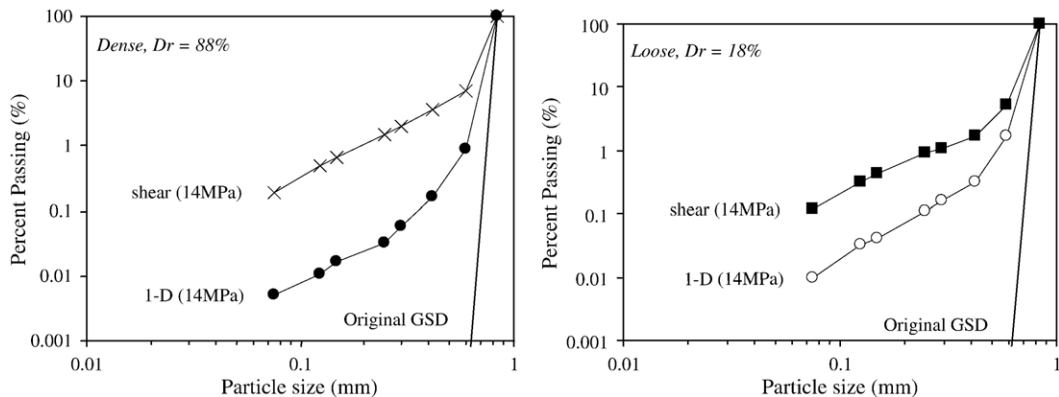


Fig. 10. Post-crushing particle size distribution curves from one-dimensional compression tests to a max stress $\sigma=14$ MPa and in simple shear tests loaded to a normal stress $\sigma=14$ MPa and subjected to a maximum shear strain $\gamma \sim 17.6\%$ (i.e., 10°). The distributions are presented in log-log scale to highlight differences.

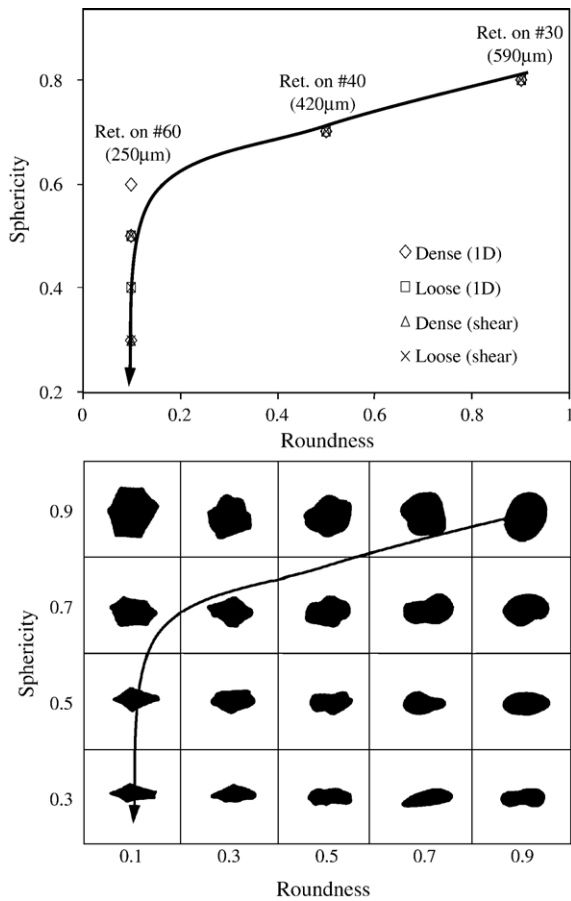


Fig. 11. Sphericity and roundness for fragments produced during crushing. The accompanying chart for sphericity and roundness is obtained from Krumbein and Sloss (1963).

prevailing fracture mechanisms that result from different loading conditions and the associated shapes of the fines produced. Coarse particles resembled the original particles and showed local contact damage and abrasion streaks, as can be seen in the SEM image in Fig. 9, or a tensile split across the diameter. Finer particles exhibited multiple fresh faces. The step-like fracture planes

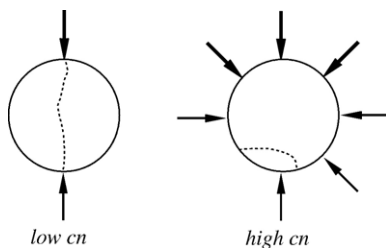


Fig. 12. Low coordination for a particle in a loose packing leads to equatorial splitting, while high coordination for a particle in a dense packing prevents equatorial splitting and leads to local crushing.

commonly observed suggest that mixed mode fractures are induced in grains within a packing.

Average sphericity and roundness values for the different fines fractions are plotted in Fig. 11. Particle sphericity and roundness decrease as the size of produced fines decreases. Eventually, the finer fractions (retained on sieves #60, #100 and #200) are flat (e.g., platy) and blade-like. This evolution of shape with size was observed in both one-dimensional and shear loading.

4.2. Discussion

The energy required to crush rock material is proportional to the amount of new surface area that is created. Therefore, energy consumption increases with fines generation, and it can be estimated that 10 times more energy is spent in producing pond screenings than in producing 10SM sand, for the same weight. It can be concluded that a very important percentage of consumed energy is spent in producing the non-commercial products.

The packing density that develops within crushers as the aggregates pass through affect the energy required to crush rock and the characteristics of the products (fines content and particle shape). The evolution of packing density is determined by choking conditions and the geometry of the crusher. The average normal contact force per particle N decreases as the number of contacts per particle (i.e., coordination number c_n) increases for the same applied stress σ . The following semi-empirical equation captures the interplay between these parameters (Santamarina et al., 2001):

$$N = \sigma \frac{12\pi}{c_n^2} D^2 \tag{1}$$

Therefore, it is estimated that the average contact force per particle in a dense packing is smaller than in a loose packing by a factor of approximately 3/4. In addition, the loading of low coordination number particles in loose

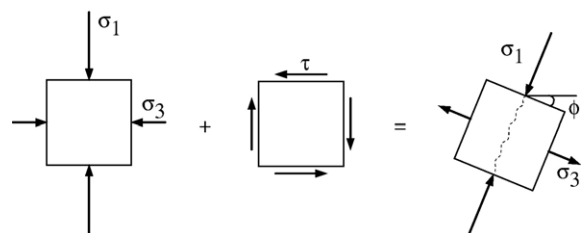


Fig. 13. Rotation and increase in principal stress when shear is applied.

packings resembles diametric point loading (weak resistance), while the loading of high coordination number particles in dense packings produces a multi-directional loading condition that solicits a stronger aggregate response (Fig. 12). These observations explain why the higher elastic yield stress σ_y measured for dense packings is twice higher than for loose packings (Fig. 8: $\sigma_{y\text{-dense}} \sim 60$ MPa and $\sigma_{y\text{-loose}} \sim 30$ MPa).

The void ratio vs. logarithm of the applied load e -log σ trends for loose and dense specimens cross in Fig. 8 at $\sigma \sim 46$ MPa and $e = 0.44$. A mechanistic interpretation suggests the following sequence of events: the loose specimen experiences crushing at a lower load, generated fines fill the voids effectively reducing the void ratio even beyond the lower initial void ratio of the dense specimen, the interparticle coordination experiences a significant increase, and the initially loose specimen becomes more stable than the dense specimen. Eventually, the two specimens asymptotically approach a similar e -log σ response at very high stress (Fig. 8).

The relative motion between the crushers' walls determines the degree of shear strain imposed on grains. The increase in fines generation with the application of shear is the result of increased principal stress (Fig. 13), increased shear force at interparticle contacts (see Rothenburg and Bathurst, 1989), the development of mixed-mode fracture propagation and higher abrasion. (Note: the shear strain is $\gamma = 18\%$ during shear loading, as compared to $\gamma \sim 2\%$ in one-dimensional loading). Furthermore, when subjected to shear, dense packings produce more fines than loose ones because (1) a higher principal stress develops in dense specimens due to the contribution of dilation to the peak shear strength and (2) asperities break during shear to overcome rotational frustration.

5. Conclusions

Site visits and an extensive survey revealed the most common characteristics among granite and carbonate crushing operations in Georgia. In addition, the analysis of previously published results and new experimental studies with single aggregates and grain packs provide support to the following conclusions:

- A large percentage of the energy required to crush rocks is spent in producing non-commercial fine-grained products.
- Single-aggregate and grain-pack crushing studies show that particle-level loading conditions determine the failure mode, resulting particle shape and fines generation.
- “Point loading” develops in single aggregates subjected to in-line, longitudinal and Brazilian loading conditions. A similar failure mode takes place in grains with low interparticle coordination within loose packings. Point loading promotes mode I fracture propagation, which generates the least amount of fines as shown by clean fracture faces on aggregates.
- Conversely, aggregates with high interparticle coordination in dense packings and single aggregates that are loaded through large contact areas experience mixed-mode fracture propagation, show evidence of micro-fracturing on new aggregate faces and generate a large amount of fines.
- The generation of fines increases with increasing shear, in both low and high interparticle coordination packings.
- The results from this study support the producers' empirical observations that unwanted fines generation and desired aggregate cubicity are mutually dependent—at least in the context of current crushing technology. In general, loading conditions that promote low coordination and mode I fracture propagation produce flaky and rod-shaped aggregates; these can be readily broken in flexural loading to improve cubicity, with minimal fines generation. On the other hand, operations that promote high coordination produce higher cubicity at the expense of increased fines generation through abrasion and asperity breakage.
- The evolution of packing density within a crusher depends on its operation and geometric design. Choke feeding promotes high coordination, favors cubicity and produces a large amount of fines.
- The analysis of aggregates produced in current crushing operations suggests that multiple loading conditions and fracture modes occur. The faces of aggregates sampled from secondary and tertiary crushers show both planar surfaces with powder (as observed in compression tests and high coordination specimens) as well as clean rough surfaces (as observed in tensile tests and low coordination specimens).

Acknowledgments

This research was conducted by the authors while at the Georgia Institute of Technology. Support was provided by Georgia crushed stone companies and The Goizueta Foundation. Results sketched in Fig. 3 were gathered in collaboration with L. Germanovich. Results in Fig. 4 were obtained by S.J. Santamarina.

References

- ASTM D 422-63, 2000. Standard test method for particle-size analysis of soils. Annual Book of ASTM Standards. Soil and Rock (I): D 420-D 5779, vol. 04.08. ASTM, Philadelphia, pp. 10–17.
- Bowers, L.R., Broaddus, W.R., Dwyer, J.J., Hines, J.D., Stansell, R.W., 1996. Processing plant principles, In: Barksdale, R. (Ed.), *The Aggregate Handbook*, Third ed. National Stone Association, Washington, pp. 8.1–8.84.
- Collins, R., Slaughter, P., Cown, M., 1997. Utilization of fines in concrete. *Stone Review* 18–22 (October).
- Coop, M.R., Sorensen, K.K., Freitas, T.B., 2004. Particle breakage during shearing of a carbonate sand. *Geotechnique* 54 (3), 157–163.
- Germanovich, L.N., Carter, B.J., Ingraffea, A.R., Dyskin, A.V., Lee, K.K., 1996. Mechanics of 3-D crack growth under compressive loads. In: Aubertin, Hassani, Mitri (Eds.), *Rock Mechanics*. Balkema, Rotterdam, pp. 1151–1160.
- Gramberg, J., 1989. *A Non-Conventional View on Rock Mechanics and Fracture Mechanics*. Balkema, Rotterdam, The Netherlands.
- Guimaraes, M., 2002. Crushed stone fines and ion removal from clay slurries—fundamental studies. PhD Dissertation, Georgia Institute of Technology.
- Hardin, B.O., 1985. Crushing of soil particles. *ASCE Journal of Geotechnical and Geoenvironmental Engineering* 111 (10), 1177–1192.
- Heikkila, P., 1991. *Acta Polytechnica Scandinavica*, Series No. 96. Helsinki, Finland, pp. 19–39.
- Joer, H.A., Bolton, M.D., Randolph, M.F., 1999. Compression and crushing behavior of calcareous soils. *International Workshop on Soil Crushability*. Yamaguchi, Japan, pp. 158–173.
- Kranz, R., 1979. Crack–crack and crack–pore interactions in stressed granite. *International Journal of Rock Mechanics and Mining Sciences and Geomechanics Abstracts* 16, 37–47.
- Krumbein, W.C., Sloss, L.L., 1963. *Stratigraphy and Sedimentation*, Second ed. W.H. Freeman and Company, San Francisco.
- Lee, K.L., Farhoomand, I., 1967. Compression and crushing of granular soils in anisotropic triaxial compression. *Canadian Geotechnical Journal* 4 (1), 68–86.
- Lee, K.L., Seed, H.B., 1967. Drained strength characteristics of sands. *Journal of the Soil Mechanics and Foundations Division, ASCE* 93 (SM6), 117–141.
- Lobo-Guerrero, S., Vallejo, L.E., 2005. Discrete element method evaluation of granular crushing under direct shear test conditions. *Journal of Geotechnical and Geoenvironmental Engineering* 131 (10), 1295–1300.
- McDowell, G.R., 1999. Micromechanics of clastic soil. *Proceedings of the International Workshop on Soil Crushability*. Ube, Yamaguchi, Japan, pp. 138–157.
- McDowell, G.R., Bolton, M.D., 1998. On the mechanics of crushable aggregates. *Geotechnique* 48 (5), 667–679.
- McDowell, G.R., Daniell, C.M., 2001. Fractal compression of soil. *Geotechnique* 51 (2), 173–176.
- McDowell, G.R., Bolton, M.D., Robertson, D., 1996. The fractal crushing of granular materials. *International Journal of Mechanics and Physics of Solids* 44 (12), 2079–2102.
- McNally, G.H., 1998. *Soil and Rock Construction Materials*. E. and FN Spon, London.
- Nakata, Y., Kato, Y., Hyodo, M., Murata, H., Hyde, A.F.L., 1999. Single particle crushing and the mechanical behavior of sand. In: Jamiolkowski, Lancellota, LoPresti (Eds.), *Pre-failure Deformation Characteristics of Geomaterials*. Balkema, pp. 221–228.
- Nakata, Y., Hyodo, M., Hyde, A.F.L., Kato, Y., Murata, H., 2001. Microscopic particle crushing and sand subjected to one-dimensional compression, *Soils and Foundations*. Japanese Geotechnical Society 44 (1), 69–82.
- Rothenburg, L., Bathurst, R.J., 1989. Analytical study of induced anisotropy in idealized granular-materials. *Geotechnique* 39 (4), 601–614.
- Santamarina, J.C., Klein, K., Fam, M., 2001. *Soils and Waves*. John Wiley and Sons, Chichester, UK.
- Sprunt, E.S., Brace, W.F., 1974. Direct observation of microcavities in crystalline rocks. *International Journal of Rock Mechanics and Mining Sciences and Geomechanics Abstracts* 11, 139–150.
- Tapponier, P., Brace, W.F., 1976. Development of stress-induced microcracks in Westerly granite. *International Journal of Rock Mechanics and Mining Sciences and Geomechanics Abstracts* 13, 103–112.
- USGS, 2000. *Minerals Yearbook, Vol. 1*. United States Geological Service. <http://www.usgs.gov/minerals/pubs/commodity/myb>.
- Valdes, J.R., 2002. Fines migration and formation damage—microscale studies. Ph.D. Dissertation, Georgia Institute of Technology.
- Vasarhelyi, B., Bobet, A., 2000. Modeling of crack initiation, propagation and coalescence in uniaxial compression. *Rock Mechanics and Rock Engineering* 33 (2), 119–139.
- Wood, S.A., Marek, C.R., 1996. Recovery and utilization of quarry by-products for use in highway construction. *3rd Annual Center for Aggregate Research Symposium*. University of Texas, Austin, Texas, pp. 1–19.
- Yamamuro, J.A., Lade, P.V., 1996. Drained sand behavior in axisymmetric tests at high pressures. *ASCE Journal of Geotechnical and Geoenvironmental Engineering* 122 (2), 109–119.
- Zingg, T., 1935. Beiträge zur Schotteranalyse. *Schweizerische Mineralogische und Petrographische Mitteilungen* 15, 38–140.